Magnetothermal Oscillations and Spin Splitting in Bismuth and Antimony†

B. McCombe* and G. Seidel
Department of Physics, Brown University, Providence, Rhode Island
(Received 18 October 1966)

A field-modulation technique for observing magnetothermal oscillations has been used to study the Fermi surfaces and spin splitting of the Landau levels in bismuth and antimony. Magnetothermal oscillations are shown to be particularly suited for such a study because of the increased relative harmonic content at low temperatures as compared to the measurement of the de Haas–van Alphen magnetization. Also, under the conditions of appreciable harmonic content it is possible to determine whether the oscillations arise from a maximum or minimum extremal area on the Fermi surface. The effective g values of the carriers appear to be in reasonable agreement with other measurements where comparison is possible, and with theory.

I. INTRODUCTION

MAGNETOTHERMAL oscillations are the de Haas–van Alphen (DHVA) type of oscillatory dependence of the temperature of a suitably thermally isolated sample on the inverse of the applied magnetic field. This phenomenon was originally observed in bismuth by Kunzler and co-workers[1] using a dc technique. More recently, the present authors,[2,3] using a field-modulation technique, and other workers,[4,5] using variations of the dc technique, have reported the observation of magnetothermal oscillations in various metals and semimetals.

In this paper we report the use of the field-modulation technique in magnetothermal oscillations for the study of the Fermi surfaces and spin splitting of the Landau levels of bismuth and antimony, thus obtaining information about the effective g values in these materials. It is believed that this is the first direct observation of spin splitting in antimony in a DHVA-type experiment. The result demonstrates the advantages of the magnetothermal technique for this type of measurement.

Bismuth and antimony are Group V semimetals which crystallize in the arsenic structure. These materials are semimetals because there is an energy overlap between the valence band and the next highest band, so that a few electrons fill small pockets in the conduction band, leaving an equal number of holes in the valence band. The resulting small number of free charge carriers, small effective masses, and long electron-lattice relaxation times make the semimetals particularly amenable to a large number of experimental techniques. Accordingly, there have been numerous experimental studies of the Fermi surfaces and conduction properties of these materials (a partial listing can be found in the bibliographies of articles in Ref. 6). There are also a number of theoretical calculations relating to the band structure of the semimetals. The most detailed of these are the pseudopotential and orthogonal-plane-wave (OPW) calculations of the band structure of antimony and arsenic by Cohen, Falicov, and others,[7–11] and the tight-binding calculations of Mase[12] for bismuth. These calculations are all in essential agreement concerning the prediction of semi-metallic behavior and the likely location of the pockets of electrons and holes in the Brillouin zone, i.e., holes near the points T and electrons near the points L (Fig. 1). The state of experimental and theoretical knowledge of the Group V semimetals up to 1964 is summarized in the proceedings of the Topical Conference on Semimetals in New York.[6]

In order to assign the exact position in the Brillouin zone and the number of ellipsoids, it is necessary to combine the band-structure results with experiment. From an examination of the published data on Bi, Jain and Koenig[13] have deduced that the electron Fermi surface consists of a set of three warped ellipsoids centered at the points L in the Brillouin zone, and the hole Fermi surface is a single ellipsoid of revolution centered at the point T in the Brillouin zone. The electron "ellipsoids" have one principal axis parallel to a binary axis (axis of two-fold rotational symmetry), but the other principal axes are tilted approximately 6° away from the trigonal and bisectrix axes, respectively, in the trigonal-bisectrix plane. The bisectrix axis (k_y) is a

† This work was supported in part by the National Science Foundation and the Advanced Research Projects Agency.
* Present address: Naval Research Laboratory, Washington, D. C.
[1] J. E. Kunzler, F. S. L. Hsu, and W. S. Boyle, Phys. Rev. **128**, 1084 (1962).
[2] B. D. McCombe and G. Seidel, Bull. Am. Phys. Soc. **9**, 264 (1964); in *Low Temperature Physics—LT9*, edited by J. G. Daunt, D. O. Edwards, F. J. Milford, and M. Yaqub (Plenum Press, Inc., New York, 1965), p. 794.
[3] G. Seidel, W. Broshar, and B. McCombe, Bull. Am. Phys. Soc. **11**, 91 (1965).
[4] M. H. Halloran and F. S. L. Hsu, Bull. Am. Phys. Soc. **10**, 350 (1965).
[5] J. Le Page, M. Garber, and F. J. Blatt, in *Low Temperature Physics—LT9*, edited by J. G. Daunt, D. O. Edwards, F. J. Milford, and M. Yaqub (Plenum Press, Inc., New York, 1965), p. 799.
[6] American Physical Society Topical Conference on Semimetals, IBM J. Res. Develop. **8**, 215 (1964).
[7] L. M. Falicov and S. Golin, Phys. Rev. **137**, A871 (1965).
[8] M. H. Cohen, L. M. Falicov, and S. Golin, IBM J. Res. Develop, **8**, 251 (1964).
[9] S. Golin, Phys. Rev. **140**, A993 (1965).
[10] L. M. Falicov and P. J. Lin, Phys. Rev. **141**, 562 (1966).
[11] P. J. Lin and L. M. Falicov, Phys. Rev. **142**, 441 (1966).
[12] S. Mase, J. Phys. Soc. Japan **13**, 434 (1958); **14**, 584 (1958).
[13] A. L. Jain and S. H. Koenig, Phys. Rev. **127**, 442 (1962).

third axis chosen to make a Cartesian set with the binary (k_x) and trigonal (k_z) axes. The angle of tilt θ_T is defined as the angle between the trigonal axis and the k_3 principal axis of the ellipsoid. θ_T is positive if the k_3 axis is obtained by rotating from the Γ-T line towards the Γ-X line and negative if the rotation is from Γ-T to Γ-L. The hole surface in bismuth has zero tilt angle.

The pseudopotential calculations of Falicov and Lin[10] for antimony indicate that the electron pockets are located at the points L in the Brillouin zone in three equivalent distorted ellipsoids (as in bismuth) having a tilt angle of maximum area of approximately $-7°$. The holes are found by these authors to be distributed in six pockets about the point T in the mirror plane σ in the Brillouin zone. The theoretical tilt angle of minimum area for these carriers is approximately $+41°$. This calculation is generally in good agreement with the DHVA measurements of Windmiller and Priestley.[14,15] Experimental values for the corresponding tilt angles of electrons (β carrier) and holes (α carriers) are $-6°$ and $+53°$, respectively. The assignment of the signs of the carriers by these authors is the reverse of the conventional assignment.[16]

In the following section the experimental technique and apparatus are discussed briefly. A discussion of the harmonic content and wave form at low temperatures for both magnetothermal and DHVA signals is presented in Sec. III. It is shown that the magnetothermal signal contains significantly more harmonic content, which permits better resolution of the spin splitting of the Landau levels. It is also shown that a careful examination of the wave form of a single oscillation provides information about the topology of the section of Fermi surface from which it arises, i.e., whether the cross-sectional area is a maximum or a minimum. Finally, results of Fermi-surface and spin-splitting measurements on bismuth and antimony are presented and discussed in Sec. IV.

II. EXPERIMENTAL

A. Experimental Technique

A physical description of the technique has been given previously, and a detailed discussion of the experimental apparatus will be presented elsewhere.[17] Hence only the salient features will be discussed at this time.

The dc magnetothermal experiments are affected in varying degrees by extraneous heat inputs to the sample such as those resulting from mechanical vibrations, fluctuations in the bath temperature, and induced eddy currents; they are also influenced by thermometer magnetoresistance.

With the field-modulation technique, the sample, instead of being thermally isolated is coupled to the bath with a relatively short relaxation time of approximately one second. A small modulating magnetic field at low audio frequency is superimposed upon the linearly swept dc field, and the temperature variation of a carbon resistance thermometer in good thermal contact with the sample is then detected synchronously with the modulating field. The short relaxation time between sample and bath serves to maintain the sample at a constant average temperature very close to that of the bath. The predominant effect of eddy currents, which produce heating at twice the modulation frequency, is removed from the signal detected at the fundamental. The effects of thermal fluctuations and noise from other sources are also greatly reduced by the narrow-band synchronous detection system.

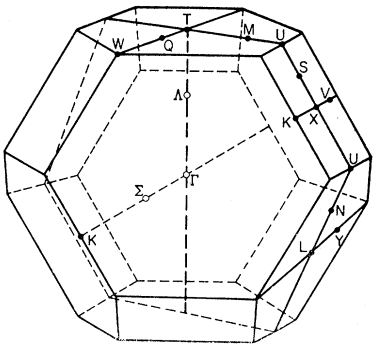

FIG. 1. Brillouin zone for the Group-V semimetals showing symmetry points and lines.

In order to make use of a field-modulation technique, certain conditions must be satisfied. In order not to damp the signal, the thermal relaxation time between sample and bath must be long compared with the inverse of the harmonic of the modulation frequency at which the signal is detected, but still short enough to maintain the average sample temperature very close to that of the bath. At the same time, the thermal relaxation time between sample and thermometer must be much less than the inverse of this same frequency; that is, the thermal contact between sample and thermometer must be good enough to ensure that the temperature of the thermometer will follow that of the sample at the detection frequency. It is also desirable for the detecting thermometer to have high sensitivity, low noise, and a small heat capacity compared with that of the sample.

The quantities measured with the field-modulation technique in magnetothermal oscillations are intimately related to quantities measured in the ordinary DHVA effect. Two configurations of dc field and modulating field were employed: (1) modulating field parallel to the dc field; and (2) modulating field normal to the dc field.

For sufficiently small modulating fields in configuration (1), the signal detected at the first harmonic (fundamental) of the modulation frequency is proportional to the rate of change of temperature with mag-

[14] L. R. Windmiller and M. G. Priestley, Solid State Commun. 3, 199 (1965).
[15] Lee R. Windmiller, Phys. Rev. **149**, 472 (1966).
[16] D. Shoenberg, Phil. Trans. Soc. (London) **A245**, 1 (1952).
[17] B. D. McCombe and G. Seidel (to be published).

netic field at constant entropy. This quantity may be written as[2]

$$\left(\frac{\partial T}{\partial H}\right)_{S,\theta} = -\frac{T}{C_{H,\theta}}\left(\frac{\partial M}{\partial T}\right)_{H,\theta}, \quad (1)$$

where T is the absolute temperature, H the magnetic field intensity, S the entropy, M the total magnetic moment, and C the total heat capacity. The angle θ measures the direction of the magnetic field with respect to a particular crystalline axis and is specifically indicated as being held constant for the case of the linearly polarized modulating field applied parallel to the dc field. In case (2), with perpendicular modulation, the signal is proportional to the rate of change of temperature with respect to angle at constant entropy and magnetic field. Using similar thermodynamic arguments, it may be shown that this quantity is related to the torque $\mathcal{T}$ by the equation

$$\left(\frac{\partial T}{\partial_{\mathrm{p}}}\right)_{S,H} = -\frac{T}{C_{H,\theta}}\left(\frac{\partial \mathcal{T}}{\partial T}\right)_{H,\theta}. \quad (2)$$

Hence it is seen that the magnetothermal oscillations in these cases are proportional to temperature derivatives of quantities usually measured in the DHVA effect.

As has been previously reported,[2] the application of both types of modulation is extremely useful in sorting out component DHVA periods from complicated patterns. In addition, the field-modulation techniques for DHVA frequency discrimination, as used by Williamson, Goldstein, and Foner[18] and by Windmiller and Priestley[14] (using variable-angle modulating field), are also applicable to magnetothermal oscillations.[17]

B. Apparatus and Samples

In order to observe DHVA-type oscillations in metals, it is generally necessary to provide sample temperatures in the range of the equilibrium temperature of liquid helium. With magnetothermal oscillations there are additional advantages in going to even lower temperatures, and hence a He^3 cryostat was constructed to provide temperatures down to 0.35°K.[19] Experiments were performed at low-magnetic fields in a standard electromagnet and at high-magnetic field in a superconducting solenoid. The field from the iron magnet was measured with a rotating-coil gaussmeter calibrated by NMR, while the field from the 85-kG solenoid was determined by measuring the current, which was also calibrated by NMR. The field-current relation was found to be reproducible to better than 1 part in 10^4, on cycling the magnet to room temperature.

The major experimental problem associated with the superconducting magnet system was the provision of a means of varying the orientation of the sample with respect to the direction of the magnet field. The rotation mechanism used was a modification of one designed by Thorsen and Berlincourt[20] and consisted of a spiral pinion gear and toothed sample holder each having a pitch of 0.047 in. The advantages of this mechanism are compactness, large gear ratio (45:1), and negligible backlash. The spiral gear, rotating sample holder, and sample-holder support were all machined from Hysol cast epoxy rod.

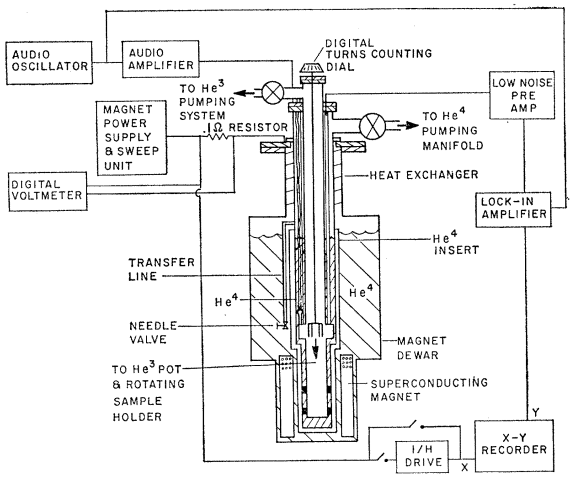

FIG. 2. Block diagram of the experimental setup.

Along the sides of the central hole in the sample holder were machined two sets of $\frac{1}{32}$-in. wide grooves such that the sample, when mounted on $\frac{3}{8}$-$\times\frac{3}{8}$-$\times\frac{1}{32}$-in. sapphire plates, could be inserted in two accurately perpendicular positions without a tedious remounting procedure. The sample holder was calibrated at room temperature with a pointer mounted on a sapphire plate and inserted in one set of grooves.

The angle between the axis of the sample holder and the axis of the support could be set with an accuracy of $\pm 0.2°$. The absolute accuracy of the setting with respect to the magnetic field is estimated to be approximately 1°.

A schematic diagram of the high-field setup, including a block diagram of the electronics, is shown in Fig. 2. The resistance variations of the temperature sensor occurring synchronously with the modulating field were converted to voltage variations by passing a small (0.1–1.0 μA), approximately constant dc current through the resistor from a current source. This ac voltage was fed into a lock-in amplifier, the dc output of which drives either a stripchart recorder or the Y axis of an X-Y recorder. The X axis of the X-Y recorder was driven by the output of a $1/H$ drive unit.[21]

The thermometers used for these measurements were

[18] A. Goldstein, S. J. Williamson, and S. Foner, Rev. Sci. Instr. **36**, 1356 (1965).
[19] G. Seidel and P. H. Keesom, Rev. Sci. Instr. **29**, 606 (1958).
[20] A. C. Thorsen and T. G. Berlincourt, Rev. Sci. Instr. **34**, 435 (1963).
[21] Paul Sullivan, Rev. Sci. Instr. **37**, 730 (1966).

0.008- to 0.010-in. slices of Allen Bradley 1/10-W nominal 11-Ω radio resistors. The Allen Bradley thermometers were prepared by grinding to the desired thickness. Fine (0.0025-in. diam.) Formvar-insulated Manganin wire leads were then soldered to the remaining bits of copper imbedded in the resistor with indium solder. Since the resulting thermometer was somewhat fragile, a mechanically strong unit was obtained by attaching the thermometer to a thin slab of sapphire with G.E. No. 7031 varnish. The sapphire slab also served as electrical insulation between the sample and the thermometer. The sensitivity of these thermometers was found to the order of $dR/dT\sim10^7$ Ω/°K at 0.35°K, at which temperature $R\sim10^6$ Ω.

Both the antimony and bismuth single crystals used were rectangular parallelepipeds with approximate dimensions 10 mm×2 mm×2 mm. Crystallographic orientations were determined by x rays to within 1°, and the measured resistivity ratios were 130 for bismuth and 2700 for antimony.

III. HARMONIC CONTENT AND WAVE FORM

A. Harmonic Content

The theory of the DHVA effect has been given by Lifshitz and Kosevitch.[22] The oscillatory total magnetic moment parallel to the applied-magnetic field arising from a single extremal cross-sectional area of the Fermi surface ($\mathcal{A}_m(E_F)$) may be written as

$$M_{\rm osc}=\left(\frac{2\pi f}{H}\right)H^{1/2}T\sum_{r=1}\frac{P_r\exp(-rX/T_{\rm H})}{r^{1/2}\sinh(rT/T_{\rm H})}\times\sin(2\pi rf/H-2\pi r\gamma\mp\pi/4). \quad (3)$$

Here,

$$P_r=-2Vk_B(e/hc)^{3/2}\left|\frac{\partial^2\mathcal{A}(E_F)}{\partial k_z^2}\right|_m^{-1/2}\cos(r\pi gm_c^*/2m_0);$$

$T_H=\beta^*H/2\pi^2k_B$; X=scattering or "Dingle" temperature; f=DHVA frequency=$ch\mathcal{A}_m(E_F)/2\pi e$; $\beta^*=e\hbar/m_c^*c$=twice the effective Bohr magneton, where m_c^* is the cyclotron effective mass; g=effective g value; m_0 =free-electron mass; γ is a phase constant which may have any value between 0 and 1/2 depending on the dispersion relation $E(k)$; and the other symbols have their usual meaning.

The main contribution to $(\partial M/\partial H)_T$ arises from the derivative of $\sin(2\pi rf/H)$ in Eq. (3).

$$\left(\frac{\partial M}{\partial H}\right)_T=-\left(\frac{2\pi f}{H}\right)^2H^{-1/2}\sum_r r^{1/2}\frac{P_r\exp(-rX/T_{\rm H})}{\sinh(rT/T_{\rm H})}\times\cos(2\pi rf/H-2\pi r\gamma\mp\pi/4). \quad (4)$$

On the other hand,

$$\left(\frac{\partial T}{\partial H}\right)_S=-\frac{T}{C_{\rm H}}\left(\frac{\partial M}{\partial T}\right)_{\rm H}=-\frac{1}{C_{\rm H}}\left(\frac{2\pi f}{H}\right)H^{1/2}T\sum_r\frac{1}{r^{1/2}}\times\left[1-\frac{rT}{T_{\rm H}}\coth\left(\frac{rT}{T_{\rm H}}\right)\right]\frac{P_r\exp(-rX/T_{\rm H})}{\sinh(rT/T_{\rm H})}\times\sin\left(\frac{2\pi rf}{H}-\frac{2\pi r\gamma\mp\pi}{4}\right). \quad (5)$$

The significance of these considerations is that, aside from the change from cosine to sine, the magnetothermal signal possesses more relative harmonic content at low temperatures or high-magnetic field than the corresponding magnetization signal. When $rT/T_H<1$ the ratio of the rth harmonic to the fundamental in $(\partial M/\partial H)_T$ is $r^{-1/2}$, while in $(\partial T/\partial H)_S$ this ratio is $r^{3/2}$.

In Fig. 3 the normalized amplitudes of the first DHVA harmonic of $(\partial M/\partial H)_T$ and $(\partial T/\partial H)_S$ and the ratios of the second and third harmonics to the first harmonic are plotted as a function of (T/T_H) at constant field H. Collision broadening has been neglected [$\exp(-rX/T_H)=1$], since it only serves to reduce further the DHVA harmonics independent of temperature and does not affect the general behavior. Below T/T_H of about 1.5, the harmonic content of the magnetothermal signal becomes appreciably larger than the corresponding harmonic content of the magnetization signal. In fact at $T/T_H=0.8$ and 0.6, the second and third harmonic amplitudes, respectively, become larger than the first harmonic amplitude of the magnetothermal signal. (The higher harmonic amplitudes will, of course, be reduced relative to the first harmonic by

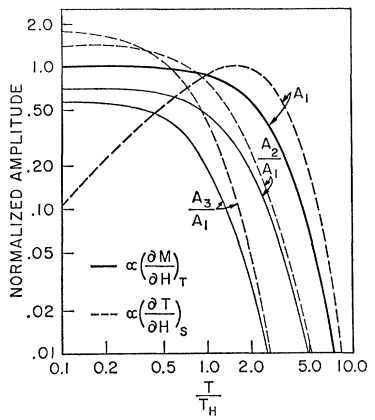

FIG. 3. Temperature dependence of the first three DHVA harmonics of $(\partial T/\partial H)_S$ and $(\partial T/\partial H)_T$. The first harmonics A_1 are plotted, as well as the ratios of the second harmonic and the third harmonic to the first harmonic, A_2/A_1 and A_3/A_1, respectively. In calculating A_1 of $(\partial T/\partial H)_S$, the heat capacity was assumed to be proportional to T. For simplicity the Dingle temperature X was taken to be zero. To obtain the influence of the collision term on the higher harmonics from the graph at a given value of T/T_H, multiply the value of A_r/A_1 by $\exp[-(r-1)X/T_H]$.

[22] I. M. Lifshitz and A. M. Kosevitch, Zh. Eksperim. i Teor. Fiz. **29**, 730 (1955) [English transl.: Soviet Phys.—JETP **2**, 636 (1956)].

the collision damping term.) This property is useful for the observation of spin splitting of the Landau levels, since the larger harmonic content makes the individual oscillations asymmetric and a great deal sharper, thus enhancing the resolution. Another interesting feature of the amplitude of the magnetothermal oscillations is that each of the harmonics exhibits an amplitude maximum as a function of temperature, and the respective amplitudes then approach zero as $T \rightarrow 0$. This is in agreement with Nernst's theorem, since the entropy (and thus $\delta T_{osc} \propto S_{sc}$) goes to zero at the absolute zero of temperature. Hence for T/T_H small (namely, much below 1), the magnetothermal signal is actually decreased. This is not the case in the ordinary DHVA effect, where the amplitude increases to a constant value as $T \rightarrow 0$ as shown in Fig. 3.

B. Wave forms

We now consider the waveforms of a single oscillation in $(\partial T/\partial H)_S$ and $(\partial M/\partial H)_T$ for the cases when the oscillation results from a maximum cross-sectional area, and when it results from a minimum cross-sectional area.

The only difference between the two cases in the expressions for the oscillatory thermodynamic quantities is in the sign of the phase factor $\pi/4$ in the argument of the sine or cosine of Eqs. (4) and (5). The minus sign is used when the area is a maximum and the plus sign when the area is a minimum.

In order to discern the effects of the two different cases on the waveform, one must be in a field and temperature regime where there is significant harmonic content. Figure 4(a) shows the theoretical wave form for $(\partial T/\partial H)_S$ using the first 8 DHVA harmonics. The parameters used were $T/T_H=0.35$, $X/T_H=0.3$, and $\cos(r g \pi m_c^*/2m_0)=1$. The constant γ was taken to be zero. The wave form for $(\partial M/\partial H)_T$, using the same number of harmonics and conditions, is shown in Fig. (4b). The difference for the cases of maximum and minimum cross-sectional areas may be seen in the direction of increasing f/H on the abscissa and the sign

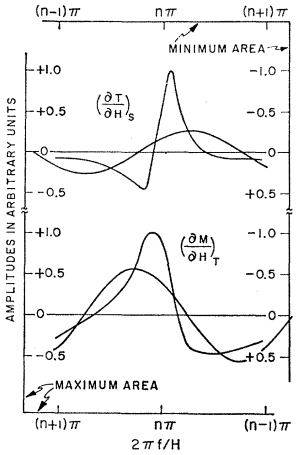

FIG. 4. Calculated wave forms including eight harmonics for a maximum (left and lower coordinates) and for a minimum (right and upper coordinates) cross-sectional area on the Fermi surface. Since curves indicate first-harmonic amplitude. The parameters used were $X/T_H=0.3$ and $T_H/T=0.35$. Spin splitting has been neglected and γ set equal to zero.

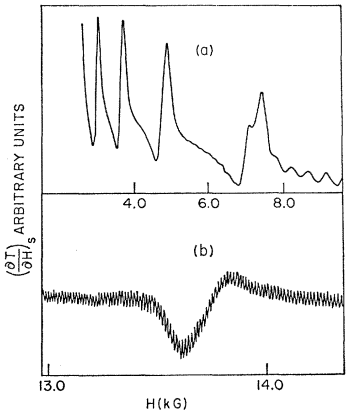

FIG. 5. Measured wave forms of $(\partial T/\partial H)_S$ at $T=0.4$°K. (a) Electrons in bismuth; (b) Hole orbits about neck of coronet in beryllium (a minimum cross-sectional area). The high-frequency oscillations arise from another piece of Fermi surface and are not of importance to the discussion.

of $(\partial T/\partial H)_S$ or $(\partial M/\partial H)_T$ on the ordinate. For the case of maximum cross-sectional area the rapidly varying portion of the curve in the $(\partial T/\partial H)_S$ signal occurs on the low-field side of the curve and the amplitude is asymmetric, being larger in the positive direction. Conversely, for a minimum cross-sectional area the rapidly varying portion occurs on the high-field side of the curve and maximum deflection occurs in the negative direction. Similar considerations apply for the $(\partial M/\partial H)_T$ signal, although the differences will be less evident at a given temperatore and magnetic field, as can be seen from the figures.

The calculated wave forms are corroborated in the case of the magnetothermal signal by the experimental curves of Fig. 5. In Fig. 5(a) is shown the observed wave form of the light electrons in bismuth with the field along the binary axis. The oscillations in bismuth, of course, result from a maximum cross-sectional area. Oscillations arising from a minimum area, the necks of the coronets in beryllium, are shown in Fig. 5(b). Such considerations should be helpful in determining the topologies of complicated surfaces.

IV. RESULTS IN BISMUTH AND ANTIMONY

A. Spin Splitting

In general the g value of conduction electrons or holes can differ from the free-electron value of 2.0023 because of spin-orbit coupling. Luttinger[23] has demonstrated that the g value can greatly *exceed* the free-electron value when there is a threefold orbital degeneracy or when the spin-orbit coupling is large compared with the energy gaps to the neighboring bands. Bismuth and antimony both satisfy the latter condition.

Cohen and Blount[24] have shown that when there is just one level immediately below the conduction band and the spin-orbit coupling is strong, the spin splitting is exactly equal to the orbital splitting. We follow Cohen

[23] J. M. Luttinger, Phys. Rev. **102**, 1030 (1956).
[24] M. H. Cohen and E. I. Blount, Phil. Mag. **5**, 115 (1960).

and Blount and define a g value by

$$g=[\lambda_1^2g_1^2+\lambda_2^2g_2^2+\lambda_3^2g_3^2]^{1/2} \tag{6}$$

and a spin-effective mass by

$$m_s^*/m_0=2/g, \tag{7}$$

where the g_i are the principal components of a symmetric second-rank tensor, and the λ_i are the direction cosines of the magnetic field with respect to the principal axes of the tensor. With these definitions, the condition that the orbital and spin splittings are equal is just that $m_s^*=m_c^*$. Here m_c^* is the cyclotron effective mass.

On the two-band model,[25] the energy levels in a magnetic field are given by

$$E_n(k_z)\left(1+\frac{E_n(k_z)}{E_g}\right)=(n+\tfrac{1}{2})\hbar\omega_c+\frac{\hbar^2k_z^2}{2m_z^*}\pm\tfrac{1}{2}g\mu_0H, \tag{8}$$

where $\omega_c=eH/m_cc^*$ is the cyclotron angular frequency, $\mu_0=e\hbar/2m_0c$ is the Bohr magneton, $m_c^*=1/(\mathbf{h}\cdot\boldsymbol{\alpha}\cdot\mathbf{h})$, $\boldsymbol{\alpha}$ is the appropriate inverse effective mass tensor, and $\mathbf{h}$ is a unit vector in the direction of the magnetic field (the z direction). The components of $\boldsymbol{\alpha}$ are taken at the bottom of the band, and all principal components are assumed much greater than 1. On this model the energy bands are nonparabolic, but surfaces of constant energy are still ellipsoidal. Cohen and Blount[24] have shown that the spin and orbital splitting of electrons in bismuth should be approximately equal for all directions where the cyclotron effective masses are much less than one. This also should be approximately valid for the conduction band of antimony.

Turning now to experimental considerations, we note that the measured quantities in a DHVA-type experiment are peak positions or peak separations in units of $1/H$. The observed peak separations need to be related to the g value or spin-effective mass. To do this, we rewrite the magnetic energy at $k_z=0$ as

$$E_n=(n+\tfrac{1}{2}\pm\Delta)\hbar\omega_c, \tag{9}$$

where

$$2\Delta=m_c^*/m_s^*. \tag{10}$$

The magnetic field at which the nth level coincides with the Fermi energy is given by

$$\frac{1}{H_{n\pm}}=(n+\tfrac{1}{2}\pm\Delta)\frac{he}{m_c^*cE_F(n\pm)}. \tag{11}$$

Since the Fermi energy may vary appreciably with magnetic field for the semimetals, E_F is written as a function of Landau level number.

For the ratio of the inverse-field separation of the spin-split peaks to the orbital separation, we may write

$$\delta\left(\frac{1}{H}\right)_{\text{spin}}\Big/\delta\left(\frac{1}{H}\right)_{\text{orbit}}=\left(\frac{1}{H_{n^+}}-\frac{1}{H_{n^-}}\right)\Big/\frac{1}{H_{n^\pm}}-\frac{1}{H_{(n-1)^\pm}}$$

$$=(n+\tfrac{1}{2})\left[\frac{1}{E_F(n^+)}-\frac{1}{E_F(n^-)}\right]+\Delta\left[\frac{1}{E_F(n^+)}+\frac{1}{E_F(n^-)}\right]\Big/(n+\tfrac{1}{2}\pm\Delta)\left[\frac{1}{E_F(n^\pm)}-\frac{1}{E_F[(n-1)^\pm]}\right]+\frac{1}{E_F[(n-1)^\pm]}. \tag{12}$$

For the conduction band in bismuth, $E_F(n^\pm)$ is replaced by $E_F(n^\pm)[1+(E_F(n^\pm)/E_g)]$ (the two-band model). In regions where the field dependence of the Fermi energy may be neglected, Eq. (11) simplifies to

$$\delta\left(\frac{1}{H}\right)_{\text{spin}}\Big/\delta\left(\frac{1}{H}\right)_{\text{orbit}}=\alpha=2\Delta. \tag{13}$$

B. Results in Bismuth

Measurements were made at both high and low fields in bismuth in the binary-trigonal plane using the apparatus described in Sec. II. DHVA periods were obtained from the low-field data by least-squares-fitting a straight line to a plot of arbitrary integer peak numbers versus peak positions in units of $1/H$. Peak positions were determined to $\pm1\%$ using field markers on the recorder chart obtained from gaussmeter readings. The estimated accuracy of the periods determined in this manner is $\pm2\%$. The peak positions at high fields were measured with an accuracy of $\pm0.5\%$, using field markers obtained from the current readings. Where resolution was good, peak separations used in the spin-splitting calculations were accurate to better than 1%.

In the measurements at low fields in bismuth and antimony, both parallel and perpendicular modulations were utilized for purposes of DHVA period discrimination. In general, first-harmonic detection was employed with modulation amplitudes small compared with peak separations. Near the binary axis in bismuth at low fields, the dominant oscillations were those due to the light-electron ellipsoids and the hole ellipsoid. Oscillations from the heavy-electron ellipsoid (principal ellipsoid) were not observable with either parallel or perpendicular modulation at low fields, and only barely resolvable at high fields. The resolution was insufficient to allow period or spin-splitting measurements.

[25] B. Lax, Bull. Am. Phys. Soc. 5, 167 (1960); B. Lax, J. G. Mavroides, H. J. Zeiger, and R. J. Keyls, Phys. Rev. Letters 5, 241 (1960).

Data concerning the angular variation of DHVA frequencies are in agreement with those of previous workers and will not be discussed in general. Only a few pictures worthy of note will be mentioned.

The experimental data for the holes fit very well to an ellipsoidal energy surface. A least-squares determination for the periods gives $(0.495\pm0.01)\times10^{-5}$ G^{-1} along the binary and $(1.53\pm0.03)\times10^{-5}$ G^{-1} along the trigonal axis for an axial ratio of 3.1 ± 0.1. This ratio should be independent of the Fermi energy provided the hole band is parabolic, and thus it should show close agreement with other experiments. The measured principal periods can be somewhat different since they depend upon the value of the Fermi energy which is very sensitive to impurities because of the small number of charge carriers (approximately 10^{-5}/atom for bismuth). Our value is slightly lower than other published values,[26–31] the difference being outside experimental error in some cases.

From the principal periods one can also obtain the number of holes *per ellipsoid*.[32] This gives $n_h=(2.88\pm0.28)\times10^{17}$/cm^3 per ellipsoid for the holes, which is an excellent agreement with the value of 2.75×10^{17}/cm^3 obtained by Smith, Baraff, and Rowell[26] (SBR) for the total number of holes and electrons on a one-hole-ellipsoid, three-electron-ellipsoid model. Brandt's[31] measurements give a value of $n_h=2.76\times10^{17}$/cm^3 while Zitter[33] obtains a value of 2.5×10^{17}/cm^3 from galvanomagnetic measurements, and Williams[30] finds $n_h=3.1\times10^{18}$/cm^3 from Alfvén-wave measurements, all in good agreement with our value.

The number of electrons per ellipsoid was not calculated because all the measurements needed to determine all the necessary parameters were not made. The experimental data for the electrons are fitted well by ellipsoidal energy surfaces in the binary-trigonal plane. The principal periods by least-squares analysis are $(6.73\pm0.13)\times10^{-5}$ along the binary and $(1.21\pm0.10)\times10^{-5}$ along the trigonal axis. The good fit to an ellipsoidal model in this plane is in agreement with Cohen's[34] nonellipsoidal nonparabolic model of the bismuth energy surfaces for band minima at L or X in the Brillouin zone, i.e., three electron ellipsoids.

SBR have made a computer fit of their high-field (88-kG) de Haas–Shubnikov data, including the effects of spin splitting and the field dependence of the Fermi energy. By varying the orbital and spin quantum numbers of the observed peaks to obtain a best fit, they were able to assign quantum numbers to the observed peaks and thus uniquely determine g values and spin masses. In what follows we shall use their published curves of the field dependence of the Fermi energy and assignment of quantum numbers in order to interpret our results.

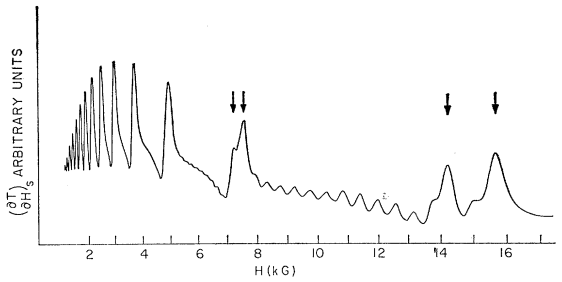

FIG. 6. Magnetothermal oscillations in bismuth with the magnetic field parallel to a binary axis. The arrows denote spin-split light-electron peaks. The higher frequency oscillations are due to the holes. $T\approx0.35$°K.

A recorder trace of magnetothermal oscillations with the magnetic field parallel to the binary axis at low fields is shown in Fig. 6. The splittings of the light-electron oscillations are resolved at about 7 and 15 kG (denoted by arrows) as observed by Kunzler *et al.*[1] The higher-frequency oscillations are due to the holes.

Some of the results of observations of spin splitting at high fields are shown in Figs. 7(a) and (b). Splitting of the hole oscillations is well resolved for values of the magnetic field along the trigonal axis down to about 18 kG. The smaller "bumps" are attributed to the electrons. Figure 7(b) shows plots of oscillations with the magnetic field along and about 2° away from the binary axis. It also demonstrates how rapidly the observed splitting increases with angle near the binary axis.

The results of our spin-splitting measurements are summarized in Table I. SBR's orbital effective masses were used in the calculation of spin masses and g values from Eqs. (7), (10), and (12). The quoted values are the average of measurements made at both low and

TABLE I. Spin-effective masses and g values for electrons and holes in bismuth. All masses are in units of the free-electron mass.

Particles	Orientation		m_c*	m_s*	g
Electrons	binary	[a]	0.0097	0.0091	220
	(light mass)	[b]		0.0089	225
	trigonal	[a]	0.065	0.11	18.2
		[b]		0.12	16.7
Holes	binary	[a]	0.21	1.5	1.3
		[b]		1.5	1.3
	trigonal	[a]	0.064	0.033	60.6
		[b]		0.034	59.3

[a] Reference 26.
[b] This work.

[26] G. E. Smith, G. A. Baraff, and J. M. Rowell, Phys. Rev. **135**, A1118 (1964).
[27] C. G. Grenier, J. M. Reynolds, and J. R. Sybert, Phys. Rev. **132**, 58 (1963).
[28] Y. Eckstein and J. B. Ketterson, Phys. Rev. **137**, A1777 (1965).
[29] Y. H. Kao, Phys. Rev. **129**, 1122 (1963).
[30] G. A. Williams, Phys. Rev. **139**, A771 (1965).
[31] N. B. Brandt, J. F. Dolgolenko, and N. N. Stupochenko, Zh. Eksperim. i Teor. Fiz. **45**, 1319 (1963) [English transl.: Soviet Phys.—JETP **18**, 908 (1964)].
[32] D. Shoenberg, in *Progress in Low Temperature Physics*, edited by C. J. Gorter (North-Holland Publishing Co., Amsterdam, 1957), Vol. II, p. 238.
[33] R. N. Zitter, Phys. Rev. **127**, 1471 (1962).
[34] M. H. Cohen, Phys. Rev. **121**, 387 (1961).

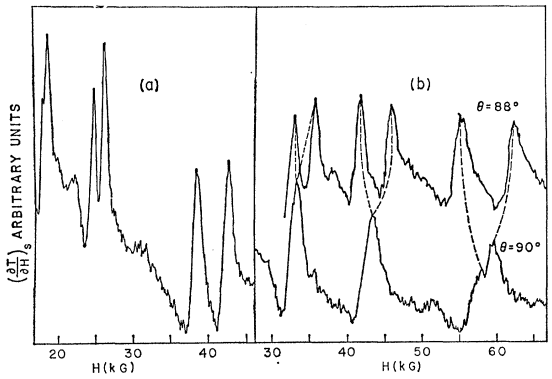

FIG. 7. Spin splitting of the holes in bismuth at high fields. (a) Magnetic field parallel to the trigonal axis; (b) magnetic field along and near the binary axis; θ is measured from the trigonal axis. $T\approx 0.4$°K.

high fields where appropriate. The results of SBR are included for comparison.

The difference between the spin and orbital effective masses along the binary axis for the light electrons (0.0089 compared to 0.0097) is a measure of the deviations from the two-band model of Cohen and Blount[24] and an indication of the effects of other bands. For this orientation the effects of other bands are indeed small (approximately 9%) and the two-band model is a good approximation. Along the trigonal axis the two-band model predicts $m_s^*=\sqrt{2}m_c^*$, while we observe $m_s^*=1.85m_c^*$, and SBR obtain $m_s^*=1.69m_c^*$; hence the effects of other bands are of the order of 20–30% in this direction.

An interesting effect of the spin splitting of the hole-energy levels observed at low fields was a vanishing of the first DHVA harmonic (fundamental) and the appearance of the second harmonic at angles of 72.5°±1° and 85.5°±1° from the trigonal axis in the binary trigonal plans. The condition for this "doubling" to occur is simply that the spin-energy splitting equal a half-integral multiple of the orbital energy splitting. This phenomenon has been observed by others[28,35] and will not be discussed further.

As pointed out by SBR and discussed above, at high field the effects of the field dependence of the Fermi energy must be considered in the measurement of DHVA periods or peak separations for spin splitting. The motion of the Fermi surface is manifested in our data by an oscillatory dependence of the hole period on magnetic field along and near the binary axis. Our results are in good agreement with the work of SBR.

C. Results in Antimony

Low-field measurements were made of the angular dependence of the DHVA periods in the binary-bisectrix plane in antimony. These we found to be in good agreement with Windmiller and Priestley[14,15] and will not be presented here. With parallel modulation the dominant oscillations at all orientations in the binary-bisectrix plane in antimony were always those having the longest DHVA period. (These oscillations were identified by Windmiller and Priestley as due to electrons.)

TABLE II. g Values of electrons and holes in antimony.

	Axis	$\hbar\omega_s \ll \hbar\omega_c$	$\hbar\omega_s \lesssim \hbar\omega_c$	$\hbar\omega_s \gtrsim \hbar\omega_c$	m_c^* [a]
Electrons	binary	3.65	15.8	23.1	0.103
	bisectrix	4.00	18.2	26.2	0.090
Holes	binary				0.080
	bisectrix	5.67	22.7	34.0	0.070

[a] Values of cyclotron masses (in units of the free-electron mass) used to calculated g values. Taken from effective-mass values given in Ref. 36.

The magnetothermal measurements in antimony give a direct observation of spin splitting of the Landau levels due to the light electrons and holes in the binary-bisectrix plane. A recorder trace of the oscillations is shown in Fig. 8. The magnetic field is parallel to the bisectrix axis and the spin-split levels are indicated by arrows.

That other possibilities, such as crystal misalignment or the presence of two crystallites, were the source of the splitting can be ruled out for a variety of experimental reasons.

The g values and spin masses were calculated from the measured splittings for the light electrons and holes in the binary-bisectrix plane from Eqs. (7), (10), and (13) using Datar's[36] published cyclotron masses. The results for the g values are presented in Table II for the bisectrix and binary axes. Since we cannot measure the relative magnitudes of the spin and orbital splittings, we have calculated the g values for the three most likely cases. Because of the complexity of the oscillations, it was only possible to measure a g value for the holes along the bisectrix axis.

From the results of the band calculations and the Fermi-surface measurements, the electron pockets in

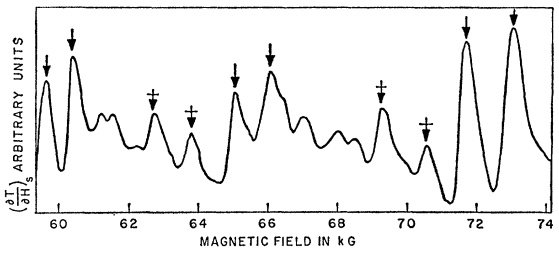

FIG. 8. Spin splitting of the light electrons and holes in antimony with the magnetic field along a bisectrix axis. The arrows denote spin-split peaks: plain for electrons; crossed for holes. $T\approx 0.4$°K.

[35] M. Suzuki and S. Kikuchi, J. Phys. Soc. Japan **19**, 134 (1964).

[36] W. R. Datars and J. Vanderkooy, I.B.M. J. Res. Develop. **8**, 247 (1964).

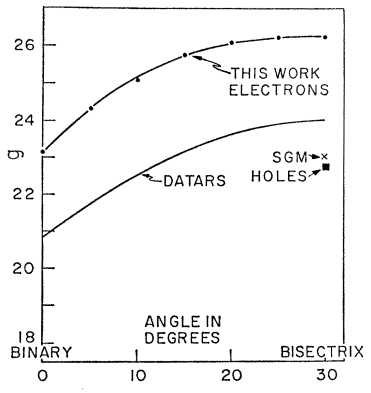

FIG. 9. Angular dependence of the g value in the binary-bisectrix plane of antimony. ●, electrons; ■, holes. Datars: see Ref. 38. SGM: see Ref. 37.

bismuth and antimony are known to be similar in both location and general form. Hence it seems likely that the only difference in their g value in the light-mass directions should result from the smaller spin-orbit interaction and larger band gap in antimony. If we make this assumption, then from the results in bismuth it seems that case 3 is the most likely.

Electron-spin-resonance measurements have been made in antimony by Smith, Galt, and Merritt[37] and by Datars.[38] Smith *et al.*, obtained for "electrons" along the bisectrix axis $g=23$. Datars measured the angular dependence of the g value of what he called electrons in the binary-bisectrix plane. Along the bisectrix axis he obtains a g valve of $g=24$; however, he also makes the statement that these carriers have a tilt angle of 36° (these would be the α carriers or holes according to Windmiller and Priestley).

Windmiller has inferred g values at various angles throughout the principal planes in antimony from a vanishing of the fundamental signal in his DHVA measurements. He finds two spin-splitting zeroes near the binary axis for the principal carrier branch and, from a comparison of Datar's g-value curve and cyclotron mass curves near the binary axis, concludes that the measured g-value curve must be that of the β carriers (electrons). This cannot be regarded as conclusive evidence, however, because of the experimental errors in the cyclotron-mass measurements.

Our own g-value measurements are plotted in Fig. 9, assuming that case 3 is correct for the electrons (β carriers). For comparison purposes, the angular variation of the g value measured by Datars is plotted on the same scale. The g value for case 2 for the holes (α carriers) is plotted at the bisectrix axis.

The discrepancy between our measurements and those of Datars is within the range of error because of the large uncertainty in the cyclotron masses. The measured spin splittings are accurate to a few percent, but the errors quoted on the cyclotron masses of Datars, which were used to calculate the g values, are larger than 10%. For example, if instead of using the Datars value of $0.090m_0$ for the electron mass along the bisectrix we use the value of $0.084m_0$ measured by Windmiller,[15] the g is changed from 26.2 to 24.4. More accurate cyclotron-mass measurements are needed to determine with better precision the g value for electrons and holes from our measurement.

Because of the smaller spin-orbit interaction and larger band gap in antimony the two-band model of Cohen and Blount[24] is expected to be less accurate for antimony than for bismuth, i.e., there should be a larger departure from $m_s^*=m_c^*$ in antimony for the light electrons. This is borne out experimentally since the deviation from this condition is only about 9% in bismuth, whereas for antimony it is 16%.

ACKNOWLEDGMENTS

It is a pleasure to acknowledge the technical assistance of Elliot Peterson. Several improvements in the apparatus were made by Wayne Broshar. One of us (BDM) would like to acknowledge financial assistance in the form of a NSF Cooperative Graduate fellowship and the permission of the Semiconductors Branch of the Naval Research Laboratory to perform one of the later experiments while employed there. He would also like to thank Dr. D. L. Mitchell for several helpful conversations.

[37] G. E. Smith, J. K. Galt, and F. R. Merritt, Phys. Rev. Letters 4, 276 (1960).
[38] W. R. Datars, Phys. Rev. **126**, 975 (1962).